Collaborative Research: Seismic and Geodetic Imaging of Subducting Terranes Under North America (S-TUNA)

Principal Investigators:
Geoffrey Abers, Boston University
Douglas Christensen and Jeff Freymueller, University of Alaska Fairbanks

Funded By NSF-EAR Geophysics

Summary. The collision of thickened crust with subduction zones significantly modifies subduction. These accretion events lead to net growth of continents and drive much of the subduction-related tectonism. Terrane collision may also have a profound effect on the size, coupling, and rupture characteristics of large intraplate earthquakes. The present accretion of exotic terranes with the Alaska subduction system represents one of the few examples of this process currently active. In this region, the collision of a region of thickened crust, the Yakutat terrane, occurs at the largest rupture asperity known, part of the 1964 Mw9.2 Alaska earthquake. The collision produces mountains along the Alaska coast and perhaps far inland, and may drive westward extrusion of distal parts of Alaska. Recently, an unusual layer, perhaps thickened crust, has been imaged at the top of the subducting plate beneath central Alaska from 70 to 150 km depth, using receiver functions from the BEAAR (Broadband Experiment Across the Alaska Range) IRIS-PASSCAL experiment. If continuous with the shallow structure, this would represent the largest deeply-subducted fragment of thickened crust yet observed. Subduction of such thick crust may help explain the size of the 1964 asperity. However, the lack of continuity between deep and shallow structures makes it difficult to tell; have these signals imaged the largest piece of thick subducted crust on the planet, or something else? In any case, what is the effect of subducting terranes on mechanics of the thrust zone?

This project images the subducted plate, upper plate, and intervening deformation in the region between the Alaska coastline and BEAAR. Here subduction passes through and past the 1964 rupture zone. Broadband seismographs image the top of the downgoing plate through and below the thrust zone. Integration with previous studies providse the longest continuous transect of a subduction zone yet available, over 700 km across strike, following a slab from the trench to coast to where last seen at 150 km depth. In parallel, a combination of geodesy and seismicity is used to image deformation currently associated with the plate interface, where it ruptured in the planet's second largest known earthquake. Modeling of deformation, when integrated with the imaging, elucidates the nature of the locked zone, the origin of the largest asperity, and the structural controls on interplate thrust processes. These results are used to test ideas for the origins of intermediate-depth earthquakes, by sampling at high resolution the transition at the down-dip end of the thrust zone in seismicity, strain, and structure.

The experiment consists of a deployment of 30 broadband seismographs at dense spacing, supplemented by short-period seismographs in places where higher-resolution seismicity would provide most information, and GPS measurements of surface deformation across this zone. Sparse permanent seismic and geodetic (PBO) stations provide regional control. Many of the seismicity and GPS sites are collocated, so there are cost savings to simultaneously conducting geodetic and seismic field work. These data, when integrated, will provide a thorough picture of terrane accretion and its impact on the generation of great earthquakes.

1. Results from Prior Support

Geoffrey Abers, Boston University

Structure of Subducting Slabs at Intermediate Depths, EAR-9725601 EAR-0096027, 5/1/98 - 4/30/02, $80,172; **CSEDI Collaborative Proposal: Thermal, Petrological, and Seismological Study of Subduction Zones**, EAR-0096028, 7/1/98-6/30/02, $17,329; EAR-0215577: $121,271, 9/1/02-8/31/05. These studies seek to understand the nature of subducted plates and in particular subducted crust. High-frequency seismic signals propagating through subducting slabs reveal that the upper 2-8 km of most subducting slabs are low-velocity layers to depths of 150-250 km, likely reflecting the persistence of hydrous phases within subducted crust well past the volcanic front [*Abers*, 2000, 2003; *Abers et al.,* 2003a]. Integration of seismology with petrologic and thermal modeling indicates that breakdown of hydrous phases induces intermediate-depth seismicity, and that seismic velocities predicted for hydrated subducted slabs resemble those observed [*Hacker et al.*, 2003a, 2003b; *Hacker and Abers*, 2003].

Jeff Freymuller, University of Alaska Fairbanks

Spatial Variations in Subduction, Kenai Peninsula, southern Alaska: EAR-9805326, $77,000. Funding Period: 7/1/98-6/30/99. J. Freymueller and S. Cohen (NASA Goddard Space Flight Center). **Coseismic, postseismic, and contemporary deformation in the 1964 Great Alaska Earthquake Rupture Zone**:. EAR-9980496, $95,375, 1/1/00-12/31/00. J. Freymueller and S. Cohen (NASA Goddard Space Flight Center). *Zweck et al.* [*2002a*] inverted velocities from survey mode GPS sites to determine which parts of the plate interface within the 1964 Alaska earthquake rupture zone were locked or slipping during 1993-1999 (Figure 5). Two separate locked patches in the shallow seismogenic zone correspond to the Prince William Sound and Kodiak asperities identified from coseismic slip models, and are separated by a region of nearly zero coupling. The present pattern of shallow coupling strongly resembles the pattern of coseismic moment release; we interpret this to mean that asperities are persistent features. The model finds significant creep up to double of the rate of plate motion occurring downdip of the entire 1964 rupture zone but not outside of it. We have generated a similar model based 35 year averaged uplift rates or angle changes that give the average rate of deformation over the entire post-1964 period [*Zweck et al.*, 2002b]. Compared to the last several years, the 35 year average model shows differences in both rate and spatial pattern of postseismic deformation. It shows rapid postseismic creep immediately downdip of the coseismic rupture, while during the last several years there has been a gap of ~70 km between the downdip end of the locked zone and the updip end of the postseismic creep [*Freymueller et al.*, 2000; *Zweck et al.*, 2002a]. *Zweck et al.* [2002b] further showed that the rates of postseismic creep over the two time periods cannot be explained by a single time-decaying process of either exponential or logarithmic form, which suggests that multiple processes were active. Tide gauge data [*Cohen and Freymueller*, 2001] show time dependent uplift rates at several sites, and provide an absolute measure of 35-year uplift rates. Four papers have been published in peer-reviewed journals [*Freymueller et al.,* 2000; *Cohen and Freymueller*, 2001; *Zweck et al.,* 2002a,b].

Douglas H. Christensen and Geoffrey Abers

Collaborative Research: Subduction, Collision, and Mountain Building, A Broadband seismic Experiment Across the Alaska Range (BEAAR). UAF: EAR97-25168, $304,752 (1/1/99 – 11/30/02). BU: EAR-9996451, $103,325 (9/1/99-11/30/03), also U. Kansas(Abers) EAR-9727183, $19,772 (12/98-8/99). *SEE Sections 3, 5:* because the results from BEAAR motivate much of the current work, the results are incorporated into the proposal body. At this stage, one year after the last data has been delivered to the IRIS Data Management Center, preliminary results have been published for the slab structure, work is completed for the crustal structure and attenuation studies and manuscripts are in their final stages, and new results on anisotropy, velocity tomography, and receiver-function migration are in progress. Abstracts and papers discuss the experiment and seismicity [*Meyers et al*., 1999a, 1999b, 1999c; *Stachnik et al*., 1999], crustal receiver functions [*Meyers et al*., 2000, 2001; *Meyers-Smith et al*., 2002], slab imaging [*Abers et al*., 2002a, b; *Ferris et al.,* 2003]; attenuation tomography and thermal structure [*Stachnik et al*., 2001, 2002a,b; *Stachnik*, 2002; *McNamara et al*., 1999; *Abers et al.,* 2003b]; anisotropy and flow [*Christensen and Abers*, 2002; *Christensen et al*., 2003]. Related studies based on these data include the first documentation of seismic events related to glacial surges [*Ekström et al.,* 2003a, b], novel use of late coda for imaging [*Campillo et al*., 2003], Lg attenuation [*McNamara*, 2000], and regional velocity tomography [*Eberhart-Phillips et al*., 2003]. One master's thesis (J. Stachnik) and senior thesis (S. Pozgay) has been completed at Boston University. One master's thesis (M. Duncan) has been completed at the University of Alaska Fairbanks, and a Ph.D. thesis (E. Meyers) is in preparation.

2. Introduction

The interaction of thickened crust with subduction zones can have a profound impact on the subduction process, modifying or even halting it. Depending upon their integrated buoyancy, terranes may accrete, subduct, or some combination of the two [*Molnar and Gray,* 1979; *Cloos*, 1993]. Despite a body of theory and ample geologic observations of terrane accretion, there are few modern examples where the process can be studied in situ (i.e., Taiwan, New Guinea, Alaska), and little is known about accretionary processes in the lower crust and mantle. Several fundamental processes depend upon how the deeper parts of terrane accretion works:

A. Terranes that accrete represent ***long-term addition of material to continents***, the end of a sequence which begins with extraction of primary melts at volcanic arcs and mantle plumes [*Taylor and McLennan*, 1985]. Much recent work on continental growth has focused on the bulk composition of oceanic arcs [*Holbrook et al.,* 1999; *Fliedner and Klemperer,* 1999; *Suyehiro et al.,* 1996], which in some cases appear too mafic to produce the continents through time [*Rudnick and Fountain,* 1995]. We have little idea if these compositions are preserved intact during accretion, or if accretion preferentially removes deeper, more mafic parts of arcs.

B Subduction of unusual material (seamounts, terranes, ridges) has a profound ***effect on the way in which the interplate thrust zone generates earthquakes***. For example, in Central America [*Husen et al*., 2002; *Protti et al*., 1995] and parts of Alaska [*Estabrook et al*., 1994], the subduction of seamounts seems to control the scale and size of large earthquakes. In Alaska, what is perhaps the largest known earthquake asperity, that of the 1964 earthquake, may be controlled by terrane subduction [*von Huene et al.,* 1999]. Subduction of a thick terrane has made the eastern end of the Alaska-Aleutian subduction zone have the shallowest dip (~3°) of any subduction zone on earth.

C. The buoyancy of thick subducting crust can drive back-arc convergence and shut off subduction, essentially serving as ***a mechanism for orogenesis above subduction***. In the Solomon Islands, collision of the Ontong Java plateau has led to arc polarity reversal in the last several Ma [*Hall*, 2002], and subduction of the Cocos Rise may have caused closure of the Panama Seaway [*Kolarsky et al*., 1995]. Beneath southern Alaska, results from BEAAR suggest that thick (11-22 km) crust may be subducting to great depth, perhaps buoying up the downgoing plate and driving mountain-building in the Alaska Range (see Section 3 below).

D. Subduction of thick blocks can ***scrape off much of the accreting sediment in accretionary wedges***, thus removing much of the material that was added to the continent. This seems to be happening in the Gulf of Alaska, where the Yakutat terrane is subducting [*Fruehn et al*., 1999]. The result profoundly alters the extent to which accretionary wedges can grow, and reverses the sign of the net accretionary-wedge mass flux to the continents.

The bottom line is that terrane subduction is critical to tectonics, generation of giant earthquakes, and long-term evolution of continents. This proposal aims to test the idea of terrane subduction in one of the few places it is suspected to presently occur, and in the place where the connection to thrust-zone processes may be most significant.

3. A New Observation from BEAAR

Our recent BEAAR project (Broadband Experiment Across the Alaska Range) illuminated the northern part of the subduction zone beneath Alaska (Figure 1), and revealed a startling feature: subducting crust (?) is visible to 150 km depth and is 14-20 km thick [*Ferris et al.*,

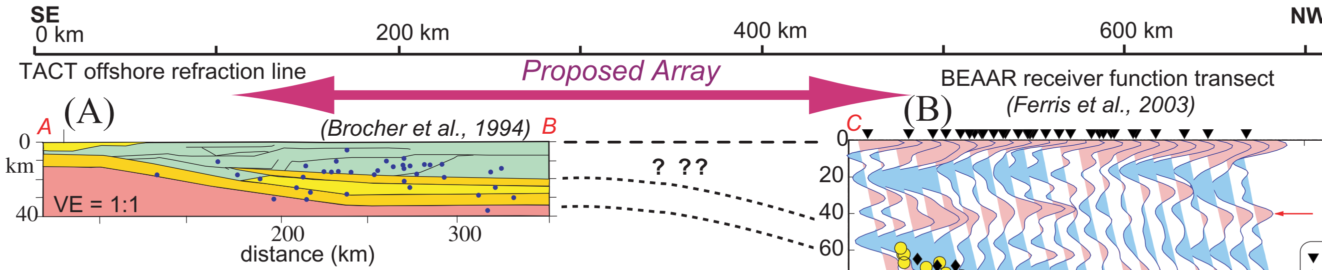

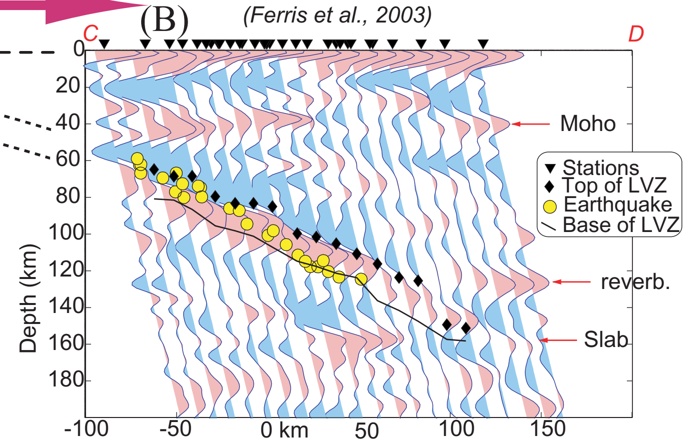

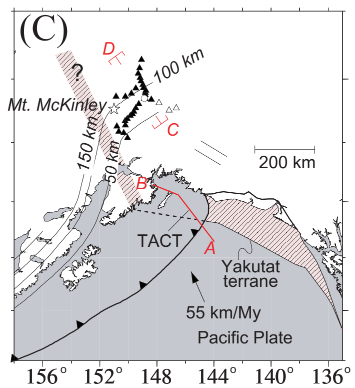

Figure 1. Cross-sections of subduction in Alaska from (A) offshore refraction, and (B) teleseismic receiver functions. (C): location map; triangles are BEAAR stations, thin lines are slab isobaths. Earthquakes are shown as dots in (A) and yellow circles in (B); the latter are relocated in the same velocity model as used in back-projecting receiver functions. For (B), colored wiggles show back-projected receiver functions along ray paths, while diamonds and thin line show top and bottom of a dipping low velocity zone (LVZ) inferred from waveform inversion.

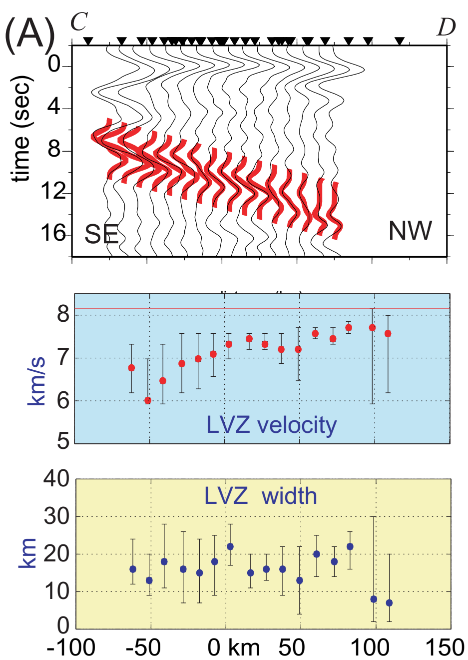

(B)

(For information, contact S. Rondenay)

http://www-eaps.mit.edu/faculty/rondenay/

Figure 2. Analyses of teleseismic scattered waves from BEAAR. (A) from *Ferris et al.* [2003], showing (top) fits to slab P-to-S conversion (red) and observed signals (thin lines), (middle) resulting estimate of thickness of LVZ, and (bottom) estimate of LVZ width. Same receiver functions and profile as Fig. 1B (NW back-azimuth). Broad, asymmetric pulses require a thick low-velocity zone. Waveform fitting is via non-linear inversion for model incorporating layer dip, with parameters being velocity, thickness, and depth of LVZ. Uncertainties are 95% confidence bounds. Note constant layer thickness but increasing velocity with increasing depth. Horizontal axis same as Figure 1B. (B) Preliminary migration of larger data set using methods of *Rondenay et al.* [2001] (courtesy S. Rondenay). Note similar thick crust, and well-defined Moho topography.

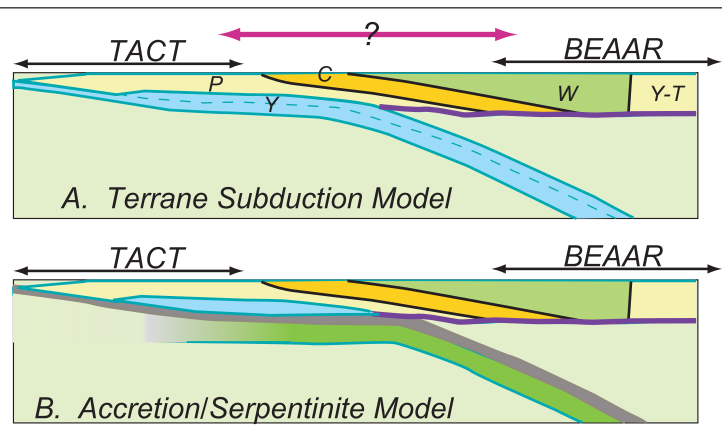

Figure 3. Two hypotheses for the origin of thick low-velocity layer seen at 70-150 km depth beneath Alaska. Labels denote terranes, P: Prince William; Y: Yakutat; C: Chugach; W: Wrangellia; Y-T: Yukon-Tanana; Gray: Pacific crust.

2003]. This inferrence comes from the pulse shapes in receiver functions, which require a thick low-velocity zone to explain them (Figure 2a). The result is being confirmed by full migration (Figure 2b; S. Rondenay, pers. comm. 2003). The thick layer is most likely the crust of a terrane recently or still being subducted at the trench, perhaps the Yakutat terrane. At the trench, the Yakutat terrane appears to be dragged down with the Pacific plate, and seismic refraction images in the Gulf of Alaska [*Brocher et al.*, 1994] show overall thickness of Yakutat plus Pacific crust similar to that of the deeper low-velocity zone.

If this interpretation is correct, then it means that crust as thick as ~15-20 km can subduct, so at least some terranes may return to the mantle rather than add to continental mass. Such thick crust should be nearly too buoyant to subduct [*Molnar and Gray,* 1979] and may be responsible for the compression that leads to mountain building in the Alaska Range, for the lack of volcanism there, for the unusually low plate dip in southern Alaska, and hence indirectly to the existence of the anomalously large asperity that slipped in the *Mw*9.2 1964 Alaska earthquake.

It is possible that the thick low-velocity zone is not unusual crust but something else, the most likely alternative being a thick serpentinite layer just below subducted oceanic crust in the downgoing plate (Figure 3). Receiver functions could not rule out this alternative [*Ferris et al.*, 2003]. In this scenario, the downgoing plate's mantle would be significantly hydrated in its upper part, perhaps by outer-rise faulting as proposed for the Nicaragua margin [*Rüpke et al.,* 2002; *Ranero et al.*, 2003]. Unfortunately, the southernmost BEAAR station lies well north of the region imaged by refraction where thick crust is known [*Brocher et al.*, 1994], so it is hard to tell whether or not the thick layer seen at 70-150 km depth is crust or lies deeper into the plate. Still, the BEAAR line illuminates perhaps the clearest imaged low-velocity channels atop slabs [compare *Yuan et al.*, 2000; *Abers*, 2000; *Matsuzawa et al.*, 1986; *Rondenay et al.*, 2001], and the relationship between intermediate-depth seismicity and structure can be easily seen.

For all these reasons, the proposed transect will provide an important link between deep Earth processes (imaged by BEAAR) and structures accessible near the surface at the southern coast of Alaska. The proposed array extends from the southernmost BEAAR stations as far south as practical, intersecting previous refraction transect and related reflection lines, so will allow continuity of structures with depth to be assessed. *When combined with previous work the transect will be by far the longest densely sampled image of a subduction zone on Earth, imaging subducted crust from the trench over 700 km inland to where the slab exceeds 150 km depth.*

4. Background and Previous Work

The Alaska Margin. Southern Alaska has been constructed throughout the Mesozoic and Cenozoic by the accretion of exotic terranes originating far to the south (Figures 3, 4) [e.g., *Saleeby*, 1983; *Schermer et al.*, 1984]. Much of the structure results from accretion of three or four major composite terranes, which docked since mid-Cretaceous [*Plafker et al.*, 1994]. The Wrangellia composite terrane (mostly Wrangellia, Peninsular and Alexander terranes, plus smaller terranes near the Denali Fault) hosts a range of late Paleozoic and early Mesozoic magmatic arcs, basement and sediment. In early Cenozoic time, the forearc accretionary complexes that make up the Chugach and Prince William Terranes accreted to the south, at the Border Ranges Fault and Contact Fault, respectively. These fault zones mark major discontinuities and have been imaged to dip at low angles northward to at least 20-25 km depth [*Fuis et al.*, 1991]. Subduction of Kula-Farallon related triple junctions, subsequent magmatism and ophiolite emplacement further modified these outboard terranes [*Haeussler et al.*, 2003; *Kusky and Young*, 1999; *Sisson and Pavlis*, 1993]. Although this summary grossly oversimplifies a complex geology, these terranes combined represent a substantial contribution to the crustal mass of North America, widening it by c. 500 km at the surface in Alaska.

The southernmost major terrane, the Yakutat terrane (YT), presently impinges on southern Alaska and lies largely offshore, separated in the north west by the Pamplona zone of deformation from the Prince William terrane [*Bruns*, 1983]. The YT basement varies in origin

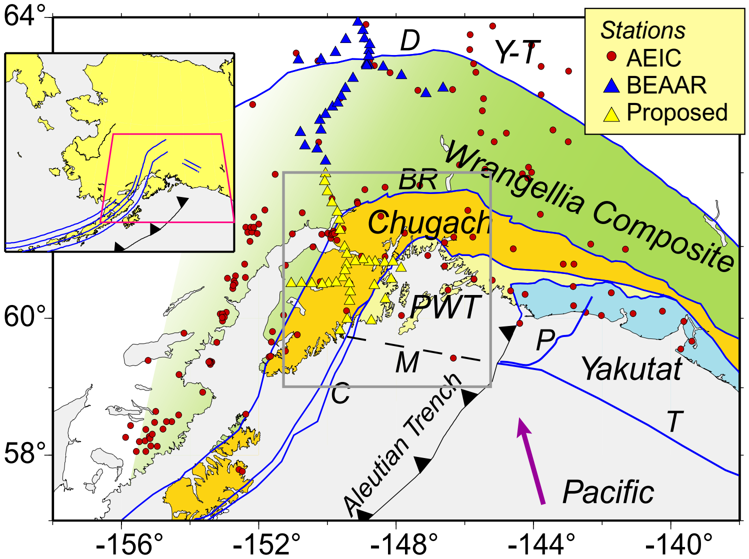

Figure 4. Southern Alaska terranes or composites, and seismic stations. PWT: Prince William Terrane; Y-T: Yukon-Tanana Terrane. Faults are D: Denali; BR: Border Ranges; C: Contact; P: Pamplona zone; T: Transition. M: Slope Magnetic Anomaly. Arrow shows direction of Pacific-North America motion, at 52 mm/yr. From *Plafker et al.* [1994] and *Brocher et al.* [1994]. Inset shows contours to slab at 50 km intervals (blue). Gray box shows location of Fig. 7.

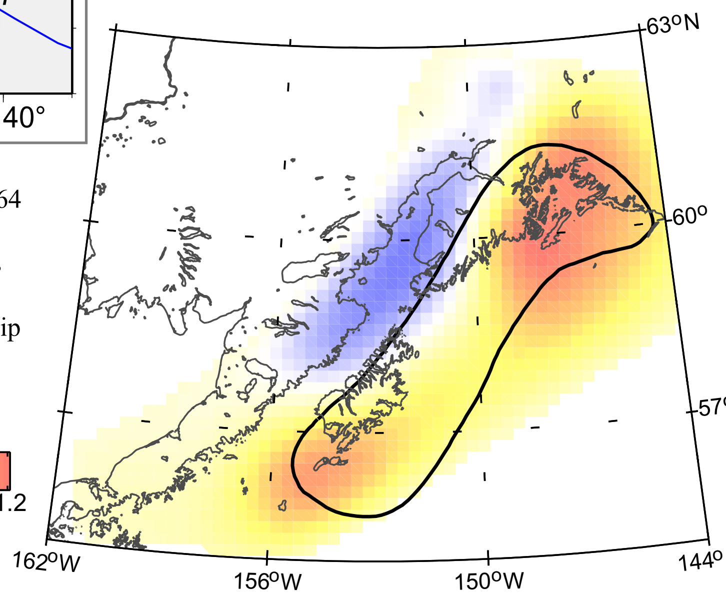

Figure 5. Plate coupling distribution from post-1964 geodetic measurements, for the preferred model of *Zweck et al.* [2002a]. The coupling is expressed as fraction of the Pacific-North American plate rate. Thick line shows 1964 earthquake rupture area. Slip in 1964 earthquake generally correlates with this coupling measurement.

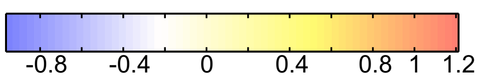

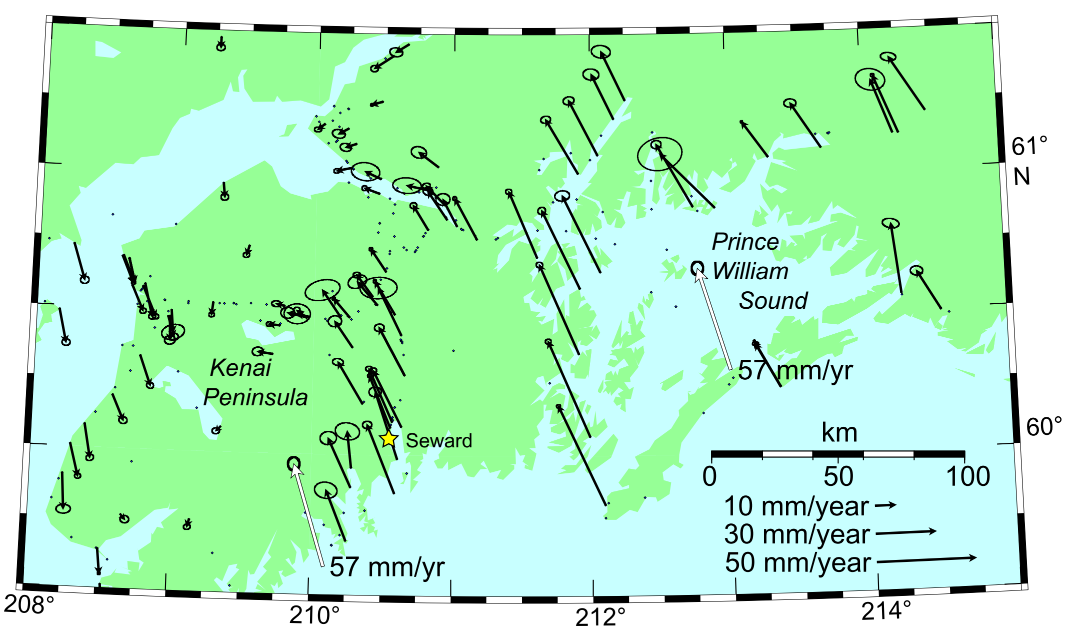

Figure 6. Horizontal velocities relative to North America measured by GPS, tipped by 95% confidence ellipses. The large white vectors show predicted NUVEL-1A relative plate motions. Note that near Seward the velocities are oriented in the direction of relative plate motions, but the azimuth of velocity vectors rotates counter-clockwise to the east across Prince William Sound to an orientation parallel to the inferred Yakutat-North America relative motion direction [*Fletcher and Freymueller*, 1999]. Small dots show GPS sites that have been surveyed at least one time.

along strike, with rocks of continental affinity in its eastern 1/3, but floored by Eocene basaltic crust of MORB and ocean island affinity beneath the eastern 2/3 [*Davis and Plafker*, 1986]. The YT appears to have completely subducted west of 145°W, and its southern, trailing edge has been identified as the Slope Magnetic Anomaly (Fig. 4) [*Griscom and Sauer*, 1990]. The YT translates northward with the Pacific plate so should be subducting, as evidenced by geologic constraints [*Plafker et al.*, 1994], upper-plate seismicity [*Doser and Brown*, 2001], geodetic measurements (see Section 5B below), and the locus of plate-boundary seismicity [*Page et al.,* 1989]. Seismic refraction images offshore show a 15-20 km thick section of crust subducting, probably oceanic YT basement overlying Pacific crust, to at least 20 km depth (Fig. 1; [*Brocher et al.*, 1994]). As discussed above, the YT may continue to >150 km depth (Fig. 1).

Prince William Sound Asperity. The 1964 Prince William Sound (PWS) earthquake is the second largest earthquake in recorded history with a moment magnitude (*Mw*) of 9.2 and a seismic moment of 8.2 x 10^{29} dyne-cm [*Kanamori*, 1977]. In most subduction zones the interplate contact zone is located off shore, beneath the accretionary prism and the continental shelf, making it very difficult to study this region in detail [*SEIZE Science Plan*, 2003]. Because of the extremely shallow dip of the subducting Pacific plate in this region, the interplate coupled zone is extremely wide (up to 250 km), and the coupled zone for the 1964 earthquake lies partly below land (Figure 5). At the downdip edge of the 1964 rupture zone the subducting slab reaches a depth of about 25-30 km.

The rupture process of the 1964 earthquake has been studied in detail using seismic [*Christensen and Beck*, 1994], geodetic [*Holdahl and Sauber*, 1994], and geodetic plus tsunami [*Johnson et al*., 1996) data. Two distinct regions of high displacement (or asperities) have been identified (Figure 5), the largest of which lies in the eastern half of the rupture area and includes the epicenter in Prince William Sound [*Ruff and Kanamori*, 1983]. A second smaller asperity is located near Kodiak Island. Up to 25 m of displacement occurred on the main asperity, what may be the largest single asperity mapped anywhere to date. While it is clear from the above studies that there were two distinct asperities, the ability to resolve their exact locations is dependent on the rather sparse data which was gathered during and shortly after the earthquake, and the technique used in the study. The seismic data were particularly poor (most stations were clipped) due to the extreme size of the event. Comparisons of the results mentioned above vary greatly, with the seismic data [*Christensen and Beck*, 1994] producing an asperity much larger than either of the other inversions [*Holdahl and Sauber*, 1994; *Johnson et al.,* 1996].

Postseismic deformation from GPS measurements in this area [*Zweck et al.*, 2002*a,b*] indicate that PWS and the eastern part of the Kenai Peninsula are currently completely locked and accumulating strain. The locked patches correspond very closely to the two asperities of the 1964 earthquake, and the present pattern of locked and creeping segments agrees with the asperities inferred from seismic data for the last great earthquakes along the 1000 km of the subduction zone for which we have data (Figure 5). This correspondence suggests that the asperities of large earthquakes are persistent features (indeed, the Nov. 2003 M7.8 earthquake in the Rat Islands appears to have re-ruptured the first asperity of the 1965 Rat Islands earthquake, further evidence for this conclusion). The GPS data constrain the location of the edge of the locked zone (or asperity) to lie beneath the eastern end of the Kenai Peninsula. GPS observations above the locked portion of the fault are moving in the direction of the Pacific plate, while stations located off the asperity on the creeping portion of the fault are moving very little. Trenchward motions observed in the western Kenai Peninsula result from continued postseismic deformation following the 1964 earthquake (Figure 6) [*Freymueller et al*., 2000; *Zweck et al.,* 2002a]. It is because of these observations that we believe we can place instruments across this boundary, sampling both above the creeping section and above the locked zone.

It has been suggested that the main PWS asperity is related to the subducting YT, which is believed to extend beneath Prince William Sound and the eastern portion of the Kenai Peninsula [*Page et al.,* 1992; *Brocher et al.*, 1994; *Fuis et al.*,1991]. The Transition Fault or Slope Magnetic Anomaly (Figure 4) can be followed under the accretionary prism adjacent to the

Kenai Peninsula [*Bruns*, 1983; *Schwab et al*., 1980]. The edge of the PWS asperity lies in the same place (Figure 5; [*Zweck et al*., 2002a]). We might expect that the down-going crust undergoes a significant and possibly dramatic change in properties between the normal Pacific plate and the Yakutat block, somehow producing the asperity. Another possibility is that the underthrusting plane is between the Yakutat block and the Pacific plate, as suggested by *Brocher et al.* [1994] and *von Huene et al.* [1999]. As discussed below, the sparseness of the permanent seismic network in Alaska does not provide sufficient constraints on earthquake depths from existing data to test these hypotheses. Efforts to resolve this question by modeling the GPS data have been hampered by uncertainty in the depth(s) of the interface(s) beneath PWS.

Downdip Limit. The downdip end of rupture here is only 25-30 km deep, much shallower than 'typical' [*Tichelaar and Ruff*, 1993]. Presumably this depth represents the transition from frictionally unstable to stable sliding [*Scholz*, 1998], either because a critical temperature is reached (350-450°C) or because weak material is encountered by the thrust (i.e. serpentinite; *Peacock and Hyndman* [1999]). Thermal models of *Oleskevich et al*. [1999] place the 350°C isotherm >100 km north of the downdip end of the rupture zone, so the authors suggest the thrust zone terminates where it crosses the upper-plate Moho and encounters serpentinite. However, the Moho observed to the north [*Meyers-Smith et al.,* 2002] and west [*Fuis et al*., 1991] are all 5-15 km deeper than the down-dip end of rupture, and a more recent thermal model [*Gutscher and Peacock*, 2003] shows higher plate-interface temperatures. More generally, it is not known whether mantle is abundantly serpentinized in plate contact regions, nor whether serpentine is velocity strengthening at mantle conditions [*Moore et al*., 1997]. Recent observations of transient slip events and related tremor-like signals suggest that fluid transients may play a key role in the transition region [*Rogers and Dreger*, 2003]. Better constraints on crustal thickness and upper-mantle velocity structure at the up-dip end of rupture would help test these models, particularly when integrated with GPS constraints on the limits of locking.

Existing seismicity data. The Alaska Earthquake Information Center (AEIC) estimates hypocenters from a ~300 station permanent network in Alaska [*Ratchkovski and Hansen,* 2002]. Most are short-period vertical instruments with very limited dynamic range imposed by analog telemetry, so provide only *P* and limited *S* travel times. While much useful information on regional seismicity has been obtained [e.g., *Page et al*., 1991], Alaska is large and ~300 stations makes for a very sparse network; station spacing is 50-100 km except on volcanoes (Figures 4, 7). The area shown in Figure 7 is roughly the size of central California from the north San Francisco Bay to Parkfield, yet contains only 26 short-period seismic stations and 5 broadband seismic stations. Figure 8 shows the 160 best-recorded hypocenters in the Kenai area in 1999, located using different velocity models. A north-dipping plate interface can be seen, but its absolute depth varies considerably (c. 8 km) depending on the velocity model, an uncertainty comparable to the inferred terrane thickness. Downgoing rays make up virtually all of this data set (because of the sparse station spacing) so predicted travel times are extremely sensitive to small velocity changes [*Gomberg et al*., 1990]. Relative relocation techniques decrease the scatter in seismicity [*Ratchkovski et al*., 1998] but provide no extra information on absolute depths. The AEIC catalog typically contains 2200-2800 events per year in the area of Figure 7, approximately 10% of which have magnitudes exceeding 2.5, typically located by 20 *P* times.

Seismic Imaging. The AEIC travel time data has allowed velocity tomography at c. 50 km resolution [*Zhao et al*., 1995], currently being refined incorporating BEAAR data [*Eberhart-Phillips et al*., 2003]. The 1995 study shows a high-velocity slab, slow mantle wedge, and limited information at crustal depths. Analog waveforms from the Kenai area also show strong secondary phases (*P-S* conversions and reflections), which indicate the existence of sharp interfaces within and below the Kenai crust [*Stephens et al*., 1990].

Recently, a few permanent broad-band stations have been deployed in southern Alaska (Figure 7). These provide the first indication of the sorts of converted-wave imaging that might be possible (Figure 9). They show that complex lower crustal structure, such as may be present where the Yakutat Terrane subducts, should be resolvable. Such structure is consistent with

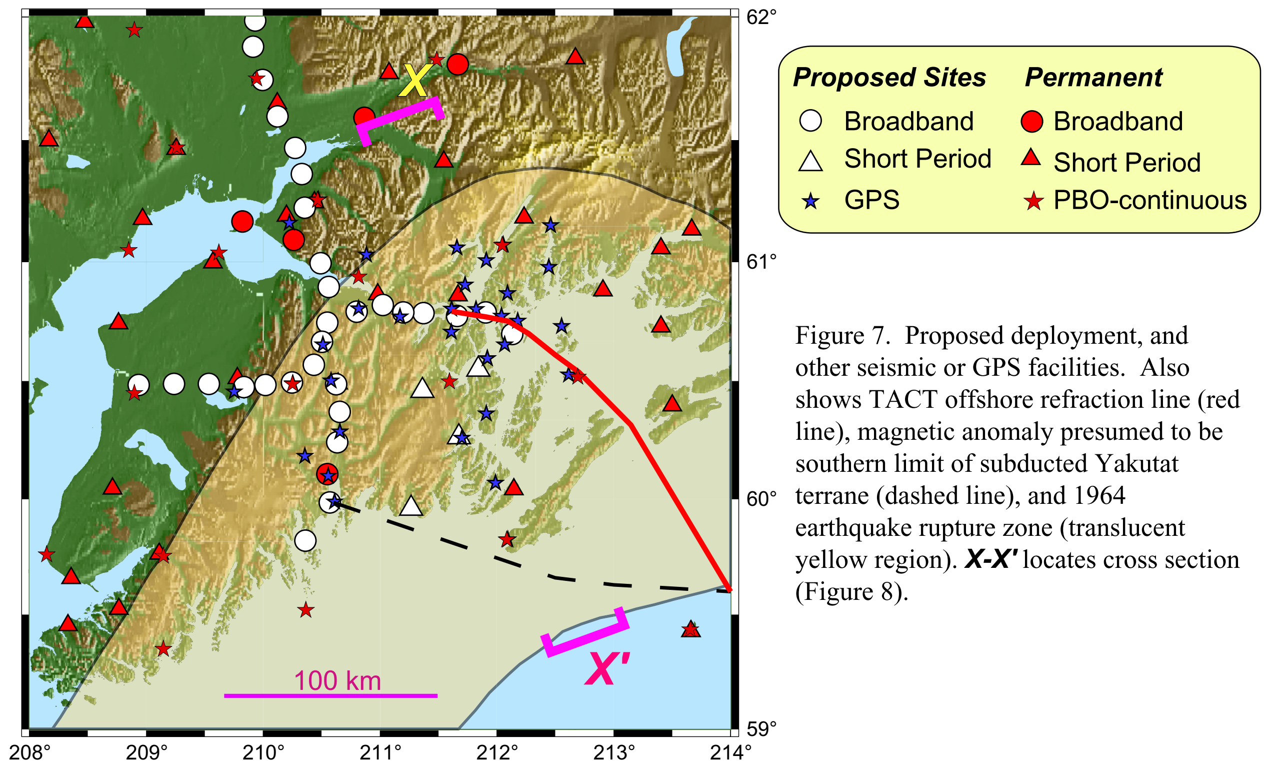

Figure 7. Proposed deployment, and other seismic or GPS facilities. Also shows TACT offshore refraction line (red line), magnetic anomaly presumed to be southern limit of subducted Yakutat terrane (dashed line), and 1964 earthquake rupture zone (translucent yellow region). ***X-X'*** locates cross section (Figure 8).

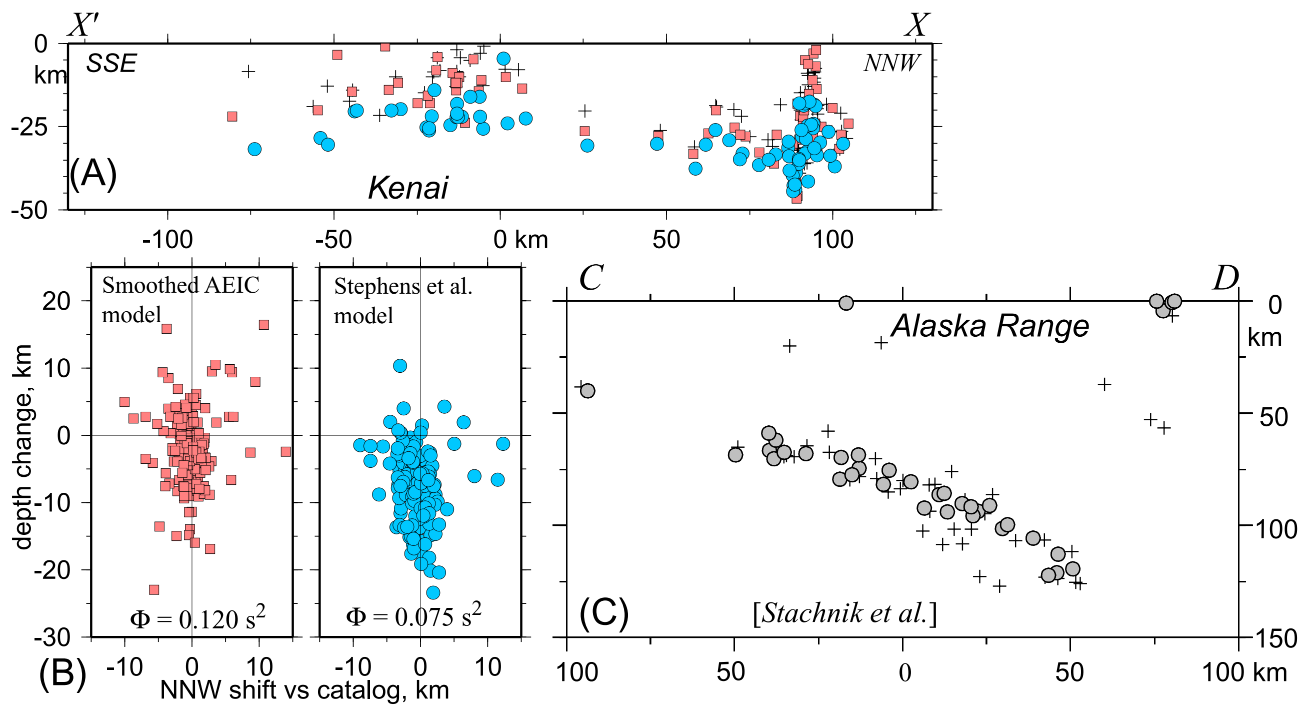

Figure 8. Hypocenter location tests. (A) Well-recorded Kenai-area seismicity for 1999 along profile *X-X'* (Fig. 6). Crosses: original AEIC catalog; orange squares: relocated in continuous approximation of AEIC velocity model; blue circles: relocated in 1D model of *Stephens et al.* [1990]. Relocation by fully nonlinear inversion [*Tartantola and Valette*, 1982], for events located by at least 15 phases. (B) Relocation vectors for events in (A) relative to AEIC catalog locations. Φ is weighted residual variance for entire data set. Note 5-15 km change in median depth with velocity model, comparable to terrane thickness. (C) Central Alaska/BEAAR cross-section *C-D* of Figure 1. Crosses: relocated with just AEIC picks; filled circles: with AEIC plus BEAAR picks. Addition of BEAAR data greatly decreases scatter of Wadati-Benioff zone seismicity.

receiver functions near Anchorage, just down-dip of the 1964 rupture zone, but considerably more complex structure is imaged further south. Because the stations are much farther apart than the volume sampled, it is impossible to conduct the kind of analysis shown on Figures 1-2 here, rendering the origin of the converters ambiguous. Some stations (not shown) sited in thick alluvial valleys show signals dominated by basin effects. Nevertheless, most data appear to be of high quality, and show that high-resolution teleseismic imaging should be possible here.

The *USArray* component of the Earthscope proposal has no concrete deployment schedule [*Earthscope Executive Committee*, 2003] but the Transportable (Bigfoot) Array is projected to move to Alaska in Years 11-12 (i.e. 2014-2015) [*Vernon et al.,* 2002]. These Alaska plans remain vague, Alaska sites are not on the current site list, and the entire state will be done in one deployment with unclear resources. As a result, this facility and its support mechanisms do not provide obvious support for the science proposed here, at least on any useful working timetable.

5. Results from recent experiments.

A. Other BEAAR results. The PI's of this proposal completed fieldwork in 2001 for the BEAAR PASSCAL array directly to the north of, and contiguous with, the array proposed here. BEAAR consisted of 36 broadband stations, deployed from 4 to 28 months, mostly along a 250 km long transect of the Alaska range at 10-15 km spacing (Fig. 1, 4). A primary goal of BEAAR is to understand what holds up North America's highest mountains (crustal thickening? heating from below?) and more generally, how subduction generates mountains. Estimates of crustal thickness from receiver functions show little change in the 35-40 km thickness across the high topography [*Meyers-Smith et al.*, 2002; Figs. 1, 2] (Figure 1B shows a complex Moho because these signals, from the north, appear to be scattered off the Denali fault; other signals show a contiguous Moho). Compensation must come from below, as seen from attenuation tomography [*Stachnik et al.,* 2002a,b; *Abers et al.*, 2003b; *Stachnik et al.*, *manuscript in internal review*, 2003], which shows a hot mantle wedge beneath the mountains. The mantle wedge looks similar in structure and Q to those of many other subduction zones. The subducted crust(?) contains all of the intermediate-depth seismicity (Fig. 1B), consistent with the notion that breakdown of hydrous minerals creates conditions necessary for earthquakes [*Hacker et al.*, 2003b].

One intriguing result is the dense anisotropy sampling from shear-wave splitting (Figure 10), which shows a sharp, 90° rotation in fast direction where slab seismicity reaches 75 km depth. Where the slab is shallower (thin mantle wedge), the fast axes align parallel to the direction of plate motion, while they are perpendicular to plate motion at greater depth (thick mantle wedge). The cause of the rotation is unclear, given standard models of mantle flow, although along-strike fast directions have been reported in other subduction zones [e.g., *Fischer et al.*, 1998]. Local shear-wave splitting data suggest that the mantle wedge contributes most to the along strike fast directions. The shallow, convergence-parallel fast directions have even less clear origin; they may be attributable to lower-plate mantle fabric, or to anisotropic upper-plate crust. In other words, do the convergence-parallel indicators record mantle flow, as commonly assumed, or do they reveal anisotropic fabric of metamorphic crustal rocks [*Brocher and Christensen,* 1990; *Godfrey et al.*, 2000]?

The BEAAR project has provided us with much experience in broadband instrumentation in Alaska, and specifically in imaging the subducting Pacific plate. The BEAAR array greatly densified the permanent monitoring network in Alaska, and earthquake locations using data from the BEAAR array are significantly more precise than standard catalog locations (Figure 8C). We can expect similar improvement in locations for the proposed deployment. We emphasize that the current project is not a continuation of the BEAAR project, as it has dramatically different goals, but it is motivated in part by the intriguing BEAAR results.

B. GPS Campaigns in Southern Alaska. The UAF Geodesy group, led by co-I Jeff Freymueller, has carried out GPS survey campaigns in southern Alaska since 1995. The principal targets for this work have been to understand the postseismic deformation following the 1964

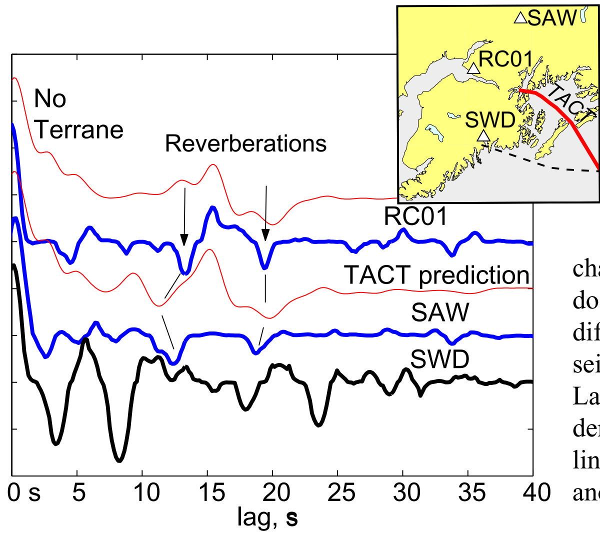

Figure 9. Preliminary stacked receiver functions (thick lines) for existing stations along proposed transect [*Llenos and Christensen*, 2003], compared with that predicted refraction structure (thin lines). *TACT prediction:* from structure imaged at northern end of TACT line of *Brocher et al.* [1994]. *No Terrane:* modified so Pacific not Yakutat crust lies at depth; large negative pulse at 10-15 s is missing. Northern stations (RC01 and SAW) show general character of TACT prediction, where Yakutat crust overlies Pacific, as do nearby BEAAR stations. Southern station SWD shows drastically different structure, perhaps related to low velocities along the seismogenic plate interface, or to high-velocity ophiolitic upper crust. Lack of correlation from SWD to RC01 is hard to understand without dense array. (Inset): site map; thick red line: TACT profile; dashed line: inferred southern limit of Yakutat terrane from magnetic anomalies.

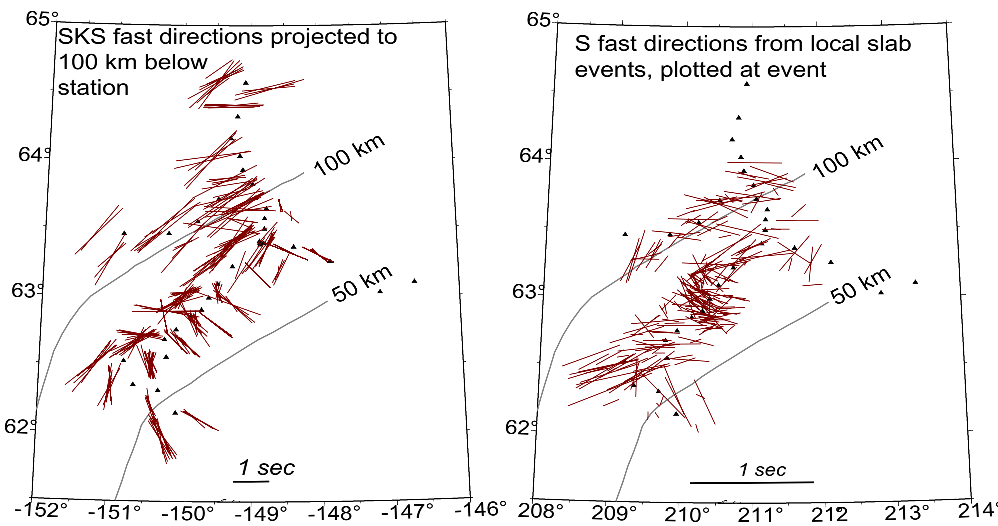

Figure 10. Shear-wave splitting results from BEAAR. Red lines denote fast directions, plotted where raypaths are 100 km deep for SKS, or at source for local events. Local raypaths used only if dominantly vertical. Gray lines show slab seismicity isobaths; triangles are stations. Rays sampling mantle wedge (slab >70 km deep) show strike-parallel fast directions, apparently from wedge. SKS shows strike-normal fast directions farther SE, possibly deeper flow or fossil fabric of downgoing plate.

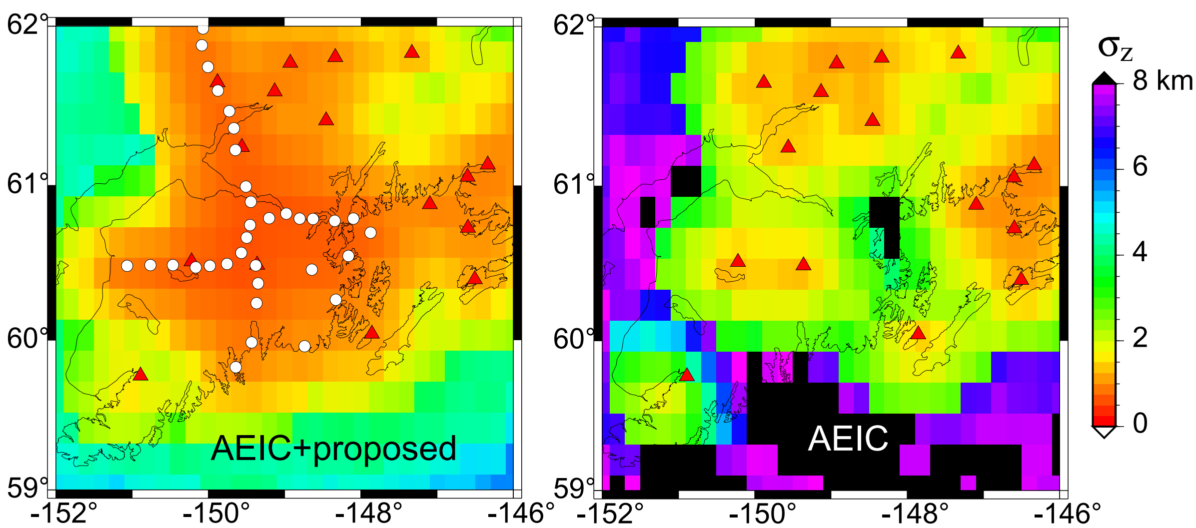

Figure 11. Location sensitivity test, showing 1-σ formal error in depth (color scale) predicted for proposed array or just permanent AEIC network. ***AEIC*** calculation assumes nominal 20 recording stations, one-third of which record S arrivals, the median reporting rate for Kenai events during 1999. The most commonly-reporting stations are used, source depth is assumed to be 25 km, and assumed a priori errors in P and S picks are 0.2 and 1.0 sec respectively. ***AEIC+Proposed*** calculation supplements these picks by P and S at all proposed sites. This linearized analysis may underestimate true errors but relative uncertainties should be well characterized, indicating that added stations improve depth accuracy by factor of 3-8 in eastern Kenai.

earthquake, the distribution of locked and slipping patches on the plate interface and its relation to the asperity distribution of great earthquakes, and slip on the Denali fault and its implications for the tectonics of southern Alaska. Including other projects in southeast Alaska and the Aleutians, we have assembled a velocity field for Alaska that included 405 sites as of the time of the 2002 Denali fault earthquake. Fig. 6 shows a subset of this data from the study area, with site velocities relative to the North American plate. This figure is significantly updated from that used by *Zweck et al*. [2002a]. One key observation that is clearly seen in the figure is the rotation of the velocity vectors across Prince William Sound. Velocity vectors in eastern Prince William Sound are oriented in the inferred Yakutat-North America relative motion direction [*Fletcher and Freymueller,* 1999, 2003], while those in western Prince William Sound are aligned in the Pacific-North American relative motion direction. This rotation of present velocities matches a similar rotation in the azimuths of 1964 coseismic slip vectors [*Parkin*, 1969], and is consistent with the idea that both the Yakutat terrane and the Pacific plate are subducting beneath North America, in slightly different directions.

Two of the goals of Freymueller's current NSF-funded project, "Mechanisms of Interseismic and Postseismic Deformation" (expires 12/2004, before this project starts) were to identify the western end of the present locked zone at the 1964 Prince William Sound asperity, and to identify the interface(s) beneath Prince William Sound that are responsible for the observed deformation. The first of these should be achieved within the next year, but the second will not be. This failure results from a combination of two factors. The first is the uncertainty in the location(s) of the interfaces, which results primarily from uncertainties in earthquake locations used to extrapolate from the TACT reflection and refraction results, and the second is the occurrence of the 2002 Denali Fault earthquake. The 2002 earthquake caused significant displacements of sites in Prince William Sound, up to a few cm, and although we did resurvey our sites in Prince William Sound as planned in 2003, this survey mainly measured earthquake displacement and did not significantly improve the site velocities. Many of the sites begun in our last NSF-funded project had only one survey before the Denali earthquake, which compromised their velocities for other purposes. Thus, most of our sites in Prince William Sound require additional data to provide a precise-enough velocity to discriminate between a model with a single subduction interface and a model with two subducting plates.

6. Goals of Proposed Project

The proposed experiment (Figure 7) is designed to answer the following specific questions, motivated by the work described above and the issues raised in the Introduction.

A. We will test the notion that the Yakutat terrane subducts continuously from the trench to 150 km depth. Similar structures have been imaged at depths below 70 km as those offshore, but using very different tools of very different resolution. Does the YT continue intact beneath the thrust zone, or are these different things? Do heterogeneities exist in layer thickness, velocity, or other, and layering? Or, alternatively, does the imaged LVZ lie below subducted crust (Fig. 3), and hence provide evidence for the hypothesis that serpentinization below subducted crust transports significant H_2O to the deeper mantle?

B. What is the relationship between thrust-zone seismicity and the Yakutat terrane? Is the thrust zone above the terrane or does the Pacific plate thrusting beneath the Yakutat terrane? Can we test the hypothesis that the 1964 Prince William Sound asperity was on the Yakutat - North America interface (the western asperity, Kodiak, was certainly on the Pacific - North America interface)? Does the geometry of terrane subduction control the location of the 1964 earthquake mega-asperity? Depth and continuity of the YT provide key constraints, as does depth of plate-interface seismicity, and the relationship of both to the plate locking geometry inferred from geodesy.

C. How does crustal fabric affect measurements of anisotropy? Strong anisotropy associated with metamorphosed terranes [*Godfrey et al.*, 2000] may dominate the upper plate in Alaska, making it a natural laboratory to test for upper-plate effects. Or does sub-plate flow dominate?

Although not primary targets, the experiment is well-suited to address the nature of deeper sources:

D. Does dehydration-induced seismicity occur beneath the thrust zone? The deeper intraslab events seem to all lie inside the subducting crust, as has been inferred elsewhere [*Hacker et al.* 2003b; *Kirby et al.,* 1996]. But does this process occur even at depths where the thrust zone is active? It might, because potentially hydrated crust is descending and warming up. Because the Yakutat crust is so thick, and may include intercalated sediment layers, this process may be particularly significant here.

E. What generates creep events and nonvolcanic tremor? We will sample a zone analogous to those where such signals have been found in SE Japan [*Obara*, 2002] and Cascadia [*Rogers and Dragert,* 2003], albeit in a colder subduction zone [*Gutscher and Peacock*, 2003]. The dense seismic array is well positioned to sample the signals, if they exist. Does the subduction of thick crust affect the occurrence of such transients? By the time of our field deployment, the EarthScope Plate Boundary Observatory (PBO) will have installed a number of continuous GPS sites aimed at detecting such transients (Fig. 7).

7. The Proposed Experiment

A. Targets and methods.

Given the questions outlined above, we have designed a data acquisition and analysis strategy to accomplish two main tasks.

(1) *We image structures* to track potential subducting terranes through and below the interplate thrust zone. This imaging will seek to establish the presence of a deeply-subducting Yakutat terrane or the alternatives discussed above, such as an abundance of hydrated mantle. The primary tool here will be teleseismic converted-wave imaging (receiver functions and their relatives). Taking advantage of experiences in BEAAR (Figures 1,2; [*Ferris et al.*, 2003]), Cascadia [*Rondenay et al.,* 2001; *Li and Nabelek*, 1999] and elsewhere [*Yuan et al.,* 2000; *Zhu*, 2000], the converted wave field will be sampled along dense 2D arrays (10-15 km spacing), to allow migration and other methods relying upon signal continuity [*Pavlis*, 2003]. Based on the observation of strong secondary phases in regional signals for the Kenai [*Stephens et al.*, 1990] and our previous experience with deeper signals [*Abers,* 2000; *Helffrich and Abers*, 1997; *Abers and Sarker*, 1996], we will supplement the teleseismic scattered-wave data with scattered local and regional signals, which should have much higher resolution albeit less uniform sampling. Also, we will sample structure through the usual variety of imaging of seismic velocities, attenuation and anisotropy.

(2) *We image strain*, through a combination of precise earthquake location and geodesy.

a) Over critical parts of the thrust zone that ruptured in 1964, we will *accurately locate microearthquake hypocenters*, by using the broadband array supplemented by short-period seismographs. These data will tell us at which depths deformation occurs. The BEAAR data (Fig. 8) confirm that nothing improves *absolute* location better than having a lot of stations nearby [also see *Thurber et al.*, 2003]. Even relative locations become much improved over those obtained from catalog arrival times (relative relocations of the AEIC catalog shows a Wadati-Benioff zone that is 10-15 km wide in central Alaska [*Ratchkovski and Hansen*, 2002], compared with c. 5 km width with the dense BEAAR network data). Resolution tests indicate that we should expect 3-8 times more accurate hypocenters in the Kenai region (Figure 11). Indeed, such improvement is necessary to test the assertion that the active plate boundary lies above not below the Yakutat block [*Page et al.,* 1989; *von Huene et al.*, 1999].

b) We will *geodetically measure strain* associated with the 1964 locked zone in the same region, and model this in terms of the geometry and extent of coupling of the locked zone. We will focus this work on the Prince William Sound region, the largest seismic asperity in North America. In particular, we will collect improved GPS velocity data, and use them to construct and compare models in which the velocities are explained in terms of locked patches either on the Pacific-North America interface, or a combination of the Yakutat-North America, Pacific-Yakutat and Pacific-North America interfaces. In order to do this, we need more accurate information about the depths and geometry of these interfaces (see above). The new GPS observations we require can be collected at almost no cost (the cost of one extra person in the field crew) while we carry out the seismic station reconnaissance, deployment, operation and removal. The major effort here, then, is in the modeling and integration of the seismic and geodetic results. Additional data from new sites of Plate Boundary Observatory (PBO) will become available over the course of this project, but the PBO network is much too sparse (typically 70-80 km spacing) to supply the dense observations we need to address the questions we have posed. These data will be useful, but cannot replace the spatially dense (and very low cost) campaign measurements we will make here. PBO will primarily provide information on transient slip on the plate boundary, and we will carefully examine both the PBO data and our seismic field data for evidence of transient slip.

Ultimately, it is *the integration of all these results* which will provide the most benefit. The scattered-wave imaging and related studies will show where the terrane boundaries are, the seismicity studies will show where at depth they may be deforming, and the geodetic analysis will show where and how the plate is coupled. Also, by integrating what could be essentially three separate projects (imaging, seismicity, geodesy), significant cost savings accrue.

B. Seismic analysis techniques

Teleseismic scattered signals. The ability to deploy dense arrays such as BEAAR has allowed scattered signals to be treated as a migratable wavefield, and various techniques have migrated *P* coda much as reflection images [e.g., *Revenaugh*, 1995; *Abers*, 1998; *Sheehan et al.,* 2000; *Rondenay et al.,* 2001; *Yuan et al.,* 2000; *Zhu*, 2000]. These studies have shown that closely-spaced arrays of receivers (~10 km) can greatly improve resolution of features at depths ranging from the mid-crust to transition zone. We plan a two-pronged approach, full 2D migration (Fig. 2b) and parameterized waveform inversion (Figs. 1, 2a). Migration provides a full image of the sample volume, while waveform inversion makes hypothesis testing feasible, and can more fully account for complex wave interactions ignored by migration [*Pavlis*, 2003]. We will continue these analyses in approaches similar to our present practice (Fig. 2). These analyses provides a primary tool for locating the plate interface, other major discontinuities, and establishing lateral variations in the velocity contrasts across them.

Conversions from regional waves. Teleseismic signals provide uniform sampling beneath arrays but provide little energy at frequencies above 1-2 Hz, so have difficulty resolving structures smaller than a few km thick. Fortunately, in subduction zones a host of high-frequency mode-converted and reflected waves have been identified and can constrain interface depth or velocities [e.g., *Matsuzawa et al.,* 1986; *Hori et al*., 1985; *Helffrich and Abers*, 1997]. Other wave propagation phenomena, such as dispersion of trapped waves, can also constrain velocity structure [*Abers*, 2000]. The shallow parts of subduction zones often show converted phases most reliably [*Matsuzawa et al*, 1986; *Hori et al.*, 1985], and clear conversions have been observed in the Kenai region [*Stephens et al.*, 1990], so this approach should be fruitful. Well recorded conversions/reflections will be migrated [e.g., *Stroujkova and Malin*, 2000].

Seismic velocities, attenuation, anisotropy. Composition, temperature, presence of fluids and melt all affect velocity and attenuation measurements. In the upper plate, *P* and *S* velocity measurements should constrain composition of crustal rocks [e.g., *Rudnick and Fountain.*, 1995]. Joint measurements of *P* and *S* travel times will allow assessment of Poisson's ratio, an indicator of serpentinization [*Christensen*, 1996] or fluid-rich zones [*Husen and Kissling*, 2001].

Attenuation measurements should provide relatively greater sensitivity to porosity/crack density at shallow depths and temperature at mantle conditions [*Mitchell*, 1995], and can be combined with velocity measurements to resolve differences between temperature and fluid effects [*Roth et al.*, 2000]. Local event tomography will image the upper plate; comparable experiments show lateral resolution better than 20 km [*Husen et al.*, 2003; *Stachnik,* 2002a,b]. Teleseismic tomography provides complementary constraints on the lower plate, although lower in resolution. We have used several approaches to velocity tomography and will experiment with the best when the data present itself [*Abers and Roecker*, 1991; *Abers*, 1994; *Zhao et al.*, 1995; *Clippard et al.*, 1995; *Searcy and Christensen*, 1994]. Body-wave attenuation can be treated similarly by measuring t^* from spectral falloff of P and S body waves, and inverting it [e.g., *Stachnik et al.,* 2002a,b]. In all of these efforts, accurate ray tracing will be necessary to correctly handle bending in a dipping slab. Modified versions of the fast Eikonal solver [*Vidale,* 1990; *Hole and Zelt*, 1995] have proven successful in dealing with slab structure thus far and have been adapted to the inversion schemes. Finally, shear-wave splitting measurements of both local and SKS phases (e.g., Fig. 10) will constrain both crustal and mantle anisotropy.

Relative and absolute hypocenters. A natural consequence of inversions of local travel times for structure are improved hypocenters, which typically are solved for jointly with velocities. We currently are implementing an inversion based on the Eikonal solvers which allows fully nonlinear earthquake location and fully three-dimensional raypaths (S. Roecker, pers. comm.; [*Thurber et al.*, 2003]), used to generate Figure 8A,B. These techniques are being adapted to incorporate both teleseismic and local travel times, either together or separately. They give absolute locations, and are complemented by relative locations using for example double-differences [e.g., *Waldhauser and Ellsworth*, 2000; *Ratchovskoi and Hansen*, 2002]. We expect several hundred locatable earthquakes within our network based on the AEIC data record over the duration of our experiment (see Existing Seismicity Data section).

C. Deployment Plan

Deployment is complicated by the long Alaska winter. The first summer we will select and prepare sites. It will be important to have the stations prepared in advance, so that the instrument deployment can be completed as early as possible during the spring of Year 2. At least 4 sites should have access to AC power and thus we will deploy 4 broadband instruments during the first summer. These four stations along with the five permanent broadband instruments already in the region will provide a broad aperture (~50-80 km) deployment for 26 months, giving baseline data over the region. During the BEAAR deployment we ran a similar broad aperture long-term subnet which provided useful records from less prolific source regions. The remaining 30 stations (26 Broadband and 4 short period; Figure 7) will be deployed during the spring of Year 2. Deployment will start when snow melts, concluding by mid to late May depending on the weather conditions. All 34 stations will run for approximately 16 months (2 summers and 1 winter). We limit remote stations to one winter because of the high cost of providing power ($1000/station per winter for air cell batteries). Our experience from BEAAR, and assessment of seismicity rates, shows that 16 months of data are clearly adequate. The easily accessible road stations will be visited periodically throughout the two summers of the deployment, and all stations will be visited in the fall of the second year and spring of the third year for normal maintenance and data gathering. In the fall of the second year all stations will be visited to install air-cell batteries for winter operation. We will monitor the more remote stations by satellite-delivered state of health messages, in order to minimize the cost of visiting the stations by boat (or float plane). In the fall of the third year (September) we will remove the stations and return them to the PASSCAL instrument center. The late (May 2005) start date is requested because the soonest PASSCAL would be able to provide this number of instruments would be 2006 or 2007 (J. Fowler, pers. comm.).

A typical field site is expected to consist of a PASSCAL-type mini-vault, with a strong emphasis on hard-rock sites. This may be very difficult in some areas, but should be possible in the southern and eastern parts of the Kenai Peninsula. Where possible, the stations will be colocated with the state microwave network (a source of power and heat), or other sites with available AC power. Most sites (~30) will be powered by deep-cycle lead-acid batteries, which can be recharged by solar panels during the summers, and by air cells during the winters. Air-cells proved to be a very reliable power source during the recent BEAAR experiment.

The University of Alaska, Fairbanks is well situated as a base for servicing the stations and management of the data. Sun workstations, large-capacity disks and DAT or Exabyte tape drives will be available for data processing, event association, and analysis. We will begin as much analysis as possible during the deployment, but we expect that fieldwork will dominate the summers during the deployment. A request has been made to PASSCAL for 34 RefTeks, 30 broadband and 4 short period sensors, sufficient disks or other storage devices, GPS receivers, and solar panels, a field computer, and miscellaneous spare parts.

GPS measurements will be made as an integrated part of the seismic array fieldwork. The stations to be surveyed are indicated by blue stars in Fig. 7. All of these sites are secure enough that a GPS receiver can be left running unattended at the site for several days, so whenever we are working in an area we will survey a few GPS sites. Setup and pickup of GPS sites will generally require less than an hour per site total. All of the sites will be surveyed one time during one of the three summers of reconnaissance, installation and operation of the PASSCAL array. In addition, about half of the sites in Prince William Sound (mostly those closest to the proposed seismic stations), will need to be surveyed twice to achieve a sufficient precision.

Data Management. As seismic data come in from the field, they will be dumped to tape and initial sorting and clock corrections will be made following PASSCAL procedures at the Geophysical Institute of the University of Alaska Fairbanks. All data will be archived at the IRIS DMC or UNAVCO following standard practice.

D. Project Management and Personnel

D. Christensen and G. Abers have extensive experience deploying and operating broadband instruments at remote sites in Alaska and elsewhere, including a recent PASSCAL experiment across the Alaska Range (BEAAR). Christensen has deployed and operated broadband instruments at remote sites in Alaska, including the Brooks Range [*Christensen et al.*, 1991], and has operated seismic networks in Alaska and Ohio. Abers has led seismic field programs throughout the world. The field deployment will be based at the Geophysical Institute of the University of Alaska Fairbanks, although portions of the field work may be based at a yet to be decided location in Anchorage, in order to be closer to the study area. Freymueller has extensive experience in carrying out GPS field surveys, and in analyzing and interpreting GPS data.

UAF will take primary responsibility for seismic data archival and GPS work (including modeling), while BU will take primary responsibility for analysis of regional signals. The full team from both institutions will collaborate on seismicity, teleseismic analyses, velocity inversions, and interpretation.

E. Broader Impact

This project includes support for 2.5 graduate students, who will benefit significantly in their education by using this project for their theses. We include support here for undergraduate interns, many of whom have in the past have come from underrepresented groups (women), and will use this project to tap additional interns from other programs (e.g. GIUAF Site REU; IRIS) to participate in fieldwork and analysis. We did this very successfully in our recent Alaska Range (BEAAR) project, and many of those interns were sufficiently motivated to go on to careers in the Earth Sciences. On a broader scale, this research provides fundamental information about the processes which generate largest earthquakes on the planet, and ultimately will lead to a better understanding of the hazard they pose to society.

REFERENCES

Abers, G.A., 1994. Three-dimensional inversion of regional P and S arrival times in the East Aleutians and sources of subduction zone gravity highs, *J. Geophys. Res., 99,* 4395-4412.

Abers, G.A., 1998. Array measurements of phases used in receiver function calculations: importance of scattering, *Bull. Seism. Soc. Am., 88*, 313-318.

Abers, G.A., 2000. Hydrated subducted crust at 100-250 km depth*, Earth and Planet. Sci. Lett., 176*, 323-330.

Abers, G.A., Seismic low-velocity layer at the top of subducting slabs beneath volcanic arcs: observations, predictions, and systematics, *Phys. Earth Planet. Int.*, *submitted*, 2003.

Abers, G.A., and S. Roecker, 1991. Deep structure of an arc-continent collision: earthquake relocation and inversion for upper mantle P and S wave velocities beneath Papua New Guinea, *J. Geophys. Res.*, *96*, 6379-6401.

Abers, G.A., and G. Sarker, 1996. Dispersion of regional body waves at 100-150 km depth beneath Alaska: In situ constraints on metamorphism of subducted crust, *Geophys. Res. Lett., 23*, 1171-1174.

Abers, G.A., B.R. Hacker and S.M. Peacock, 2001. Seismic Evidence Relating Intraslab Earthquakes to Dehydration of Subducted Crust: El Salvador, Olympia, and Elsewhere, *EOS Trans. AGU, 82*, Spring 2001 Meeting Suppl.

Abers, G.A., J. Stachnik, S. Pozgay, D.H. Christensen, R. Hansen, and E.V. Meyers, 2002a. The BEAAR Facts: Sampling the Alaska Slab, Wedge and Mountains with a Broadband Experiment Across the Alaska Range (BEAAR), *Seism. Res. Lett, 73*, 2, 219, 2002a.

Abers, G.A., A. Ferris, D. Christensen and E. Meyers-Smith, The Alaska slab imaged: Results from BEAAR, *EOS Trans. AGU*, *83(47)*, fall mtg. suppl., Abstr. S52A-1071, 2002b.

Abers, G.A., T. Plank and B.R. Hacker, 2003. The wet Nicaragua slab, *Geophys. Res. Lett*., *Geophys. Res. Lett*., *30*(2), 1098, doi: 10.1029/2002GL015649, 2003a.

Abers, G.A.,, J.C. Stachnik. and D.H. Christensen, Constraints on the Mechanism of Attenuation and Thermal Structure in Subduction Zones: Results from BEAAR, *EOS Trans. AGU Fall Meet. Suppl.*, 2003b.

Brocher, T.M., and N.I. Christensen, Seismic anisotropy due to preferred mineral orientation observed in shallow crustal rocks in southern Alaska, *Geology*, *18*, 737-740, 1990.

Brocher, T.M., G.S. Fuis, M.A. Fisher, G. Plafker, M.J. Moses, J.J. Taber, and N.I. Christensen, Mapping the megathrust beneath the northern Gulf of Alaska using wide-angle seismic data, *J. Geophys. Res.*, *99*, 11,663-11,685, 1994.

Bruns, T.R., 1983. Model for the Origin of the Yakutat Block, an Accreting Terrane in the Northern Gulf of Alaska, *Geology, 11*, 718-721.

Campillo, M., E. Larose, L. Margerin, A. Paul, B. van Tiggelen , A. Derode, and G. Abers, Empirical Synthesis of Green functions from the correlation of diffuse waves, *EOS Trans. AGU Fall Meet. Suppl.*, 2003.

Christensen, D.H., and S.L. Beck, 1994. The Rupture Process and Tectonic Implications of the Great 1964 Prince William Sound Earthquake, *Pageoph, 142*, 29-53.

Christensen, D.H., C.K. Searcy, S. Spitzak, and M. Savage, 1991. Velocity Structure and Anisotropy of the Crust and Upper Mantle in the Brooks Range, Alaska From Teleseismic Observations, EOS, 72, 296. (Fall AGU 1991)

Christensen, D. and G.A. Abers, S-wave splitting observations across the Alaska Range: Results from BEAAR, *EOS Trans. AGU*, *83(47)*, fall mtg. suppl., Abstr. S52A-1072, 2002.

Christensen, D.H., G.A. Abers, and T. McNight, Mantle Anisotropy Beneath the Alaska Range Inferred From S-wave Splitting Observations: Results From BEAAR, *EOS Trans. AGU Fall Meet. Suppl.*, 2003.

Christensen, N.I., Poisson's ratio and crustal seismology, *J. Geophys. Res.*, *101*, 3139-3157, 1996.

Clippard, J.D., D.H. Christensen, and R.D. Rechtien, 1995. Composite Distribution Inversion Applied to Crosshole Tomography, *Geophysics, 60*, 1283-1294.

Cloos, M., Lithospheric buoyancy and collisional orogenesis; subduction of oceanic plateaus, continental margins, island arcs, spreading ridges, and seamounts, *Bull. Geol. Soc. Amer.*, *105*, 715-737, 1993.

Cohen, S. C., and J. T. Freymueller, Crustal uplift in the southcentral Alaska subduction zone: A new analysis and interpretation of tide gauge observations, *J. Geophys. Res.*, *106*, 11,259-11,270, 2001.

Davis, A.S., and G. Plafker, Eocene basalts from the Yakutat terrane: Evidence for the origin of an accreting terrane in southern Alaska, *Geology*, *14*, 963-966, 1986.

Doser, D.I., and W.A. Brown, 2001. A study of historic earthquakes of the Prince William Sound, Alaska, region, *Bull. Seism. Soc. Am.*, *91*, 842-857.

Earthscope Executive Committee, EarthScope: Acquisition, Construction, Integration and Facility Management, MREFC Proposal, http://www.earthscope.org/assets/es_parts_I-IV_lo_1.25.pdf, 2003.

Eberhart-Phillips, D., D.H. Christensen, T.M. Brocher, U. Dutta, R. Hansen, and N.A. Ratchovski, Imaging the transition from Aleutian subduction to Yakutat collision in central Alaska, with local earthquakes and active source data, *Eos Trans. AGU, 84(46)*, Fall Meet. Suppl., Abstr. S21C-01, 2003.

Ekström, G., M. Nettles and G.A. Abers, Glacial earthquakes, *Science, 302,* 622-624, 2003a.

Ekström, G., M. Nettles, and G. Abers, Glacial earthquakes, *EOS Trans. AGU Fall Meet. Suppl.*, 2003b.

Estabrook, C.H., K.H. Jacob, and L.R. Sykes, Body wave and surface wave analysis of large and great earthquakes along the eastern Aleutian arc, 1923-1993: Implications for future great events, *J. Geophys. Res.*, *99*, 11,643-11,662, 1994.

Ferris, A., G.A. Abers, D.H. Christensen and E. Veenstra, High resolution image of the subducted Pacific (?) plate beneath central Alaska, 50-150 km depth, *Earth Planet. Sci. Lett., 214*, 575-588*,* 2003.

Fischer, K.M., M.J. Fouch, D.A. Wiens, and M.S. Boettcher, Anisotropy and flow in Pacific subduction zone back-arcs, *Pure and Applied Geophysics*, *151* (2-4), 463-475, 1998.

Fletcher, H., and J. T. Freymueller, New GPS constraints on the motion of the Yakutat block, *Geophys. Res. Lett., 26*, 3029-3032, 1999.

Fletcher, H. J., and J. T. Freymueller, New constraints on the motion of the Fairweather fault, Alaska, from GPS observations, Geophys. Res. Lett., 30(3), 1139, doi:10.1029/2002GL016476, 2003.

Fliedner, M., and S.L. Klemperer, Structure of an island arc: wide-angle seismic studies in the eastern Aleutian Islands, Alaska., *J. Geophys. Res..* ***104***, 10,667-10,694, 1999.

Freymueller, J. T., S. C. Cohen, and H. J. Fletcher, Spatial variations in present-day deformation, Kenai Peninsula, Alaska, and their implications, *J. Geophys. Res.*, *105*, 8079-8101, 2000.

Fruehn, J., R. von Huene, and M.A. Fisher, Accretion in the wake of terrane collision: The Neogene accretionary wedge off Kenai Peninsula, Alaska, *Tectonics*, *18*, 263-277, 1999.

Fuis, G.S., E.L. Ambos, W.D. Mooney, N.I. Christensen, and E. Geist, Crustal structure of accreted terranes in southern Alaska, Chugach mountains and Copper River basin, from seismic refraction results, *J. Geophys. Res.*, *96*, 4187-4227, 1991.

Godfrey, N.J., N.I. Christensen, and D.A. Okaya, Anisotropy of schists: Contribution of crustal anisotropy to active source seismic experiments and shear wave splitting observations, *J. Geophys. Res.*, *105*, 27991-28007, 2000.

Gomberg, J.S., K.M. Shedlock, and S.W. Roecker, The effect of S-wave arrival times on the accuracy of hypocenter estimation, *Bull. Seismol. Soc. Amer.*, *80*, 1605-1628, 1990.

Griscom, A., and P.E. Sauer, Interpretation of magnetic maps of the northern Gulf of Alaska, with emphasis on the source of the Slope anomaly, *U.S.Geol. Surv. Open-File Rep.*, *90-348*, 18 pp., 1990.

Gutscher, M.-A., and S.M. Peacock, Thermal models of flat subduction and the rupture zone of great subduction earthquakes, *J. Geophys. Res.*, *108* (B1), 2009, doi: 10.1029/ 2001JB000787, 2003.

Hacker, B.R., G. A. Abers, and S.M. Peacock, Subduction Factory 1. Theoretical mineralogy, density, seismic wave speeds, and H_2O content, *J. Geophys. Res., 108*(B1), 2029, doi:10.1029/2001JB001127, 2003a.

Hacker, B.R., S.M. Peacock**,** G. A. Abers**,** and S.D. Holloway, Subduction Factory 2. Intermediate-depth earthquakes in subducting slabs are linked to metamorphic dehydration reactions, *J. Geophys. Res., 108*(B1), 2030, doi:10.1029/2001JB001129, 2003b.

Hacker, B.R., and G.A. Abers, Subduction Factory 3. An Excel worksheet and macro for calculating the densities, seismic wave speeds, and H2O contents of minerals and rocks at pressure and temperature, *Geochem. Geophys. Geodyn. (G3)*, *submitted*, 2003.

Haeussler, P.J., D.C. Bradley, R.E. Wells, and M.L. Miller, Life and death of the Resurrection plate: Evidence for its existence and subduction in the northeastern Pacific in Paleocene-Eocene time, *Bull. Geol. Soc. Amer.*, *115*, 867-880, 2003.

Hall, R., Cenozoic geological and plate tectonic evolution of SE Asia and the SW Pacific: computer-based reconstructions, model and animations, *J. Asian Earth Sci.*, *20*, 353-431, 2002.

Helffrich, G., and G.A. Abers, 1997. Slab low-velocity layer in the eastern Aleutian subduction zone, *Geophys. J. Int.*, *130*, 640-648.

Holbrook, W.S., D. Lizarralde, S. McGeary, N. Bangs, and J. Diebold, Structure and composition of the Aleutian island arc and implications for continental crustal growth., *Geology*, ***27***, 31-34, 1999.

Holdahl, S.R., and J.M. Sauber, 1994. Coseismic slip in the 1964 Prince William Sound Earthquake: A New Geodetic Inversion, *Pageoph., 142*, 55-82.

Hole, J.A., and B.C. Zelt, 3-D finite-difference reflection travel times, *Geophys. J. Int.*, *121*, 427-434, 1995.

Hori, S., H. Inoue, Y. Fukao, and M. Ukawa, 1985. Seismic detection of the untransformed "basaltic" oceanic crust subducting into the mantle, *Geophys. J. R. astr. Soc.*, *83*, 169-197.

Husen, S., and E. Kissling, Postseismic fluid flow after the large subduction earthquake of Antofagasta, Chile, *Geology*, *29*, 847-850, 2001.

Husen, S., E. Kissling, and R. Quintero, Tomographic evidence for a subducted seamount beneath the Gulf of Nicoya, Costa Rica; the cause of the 1990 Mw = 7.0 Gulf of Nicoya earthquake, *Geophys. Res. Lett.*, *29* (8), 2002.

Husen, S., R. Quintero, E. Kissling, and B. Hacker, Subduction-zone structure and magmatic processes beneath Costa Rica constrained by local earthquake tomography and petrological modelling, *Geophys. J. Int.*, *155*, 11-32, 2003.

Johnson, J.M., K. Satake, S.R. Holdahl, J. Sauber, 1996. The 1964 Prince William Sound earthquake: Joint inversion of tsunami and geodetic data, *J. Geophys. Res., 101*, 523-532.

Kanamori, H., 1977. The Energy Release in Great Earthquakes, *J. Geophys. Res., 82*, 2981-2987.

Kirby, S., E.R. Engdahl, and R. Denlinger, Intermediate-depth intraslab earthquakes and arc volcanism as physical expressions of crustal and uppermost mantle metamorphism in subducting slabs, in *Subduction: Top to Bottom, Geophysical Monograph 96*, edited by G.E. Bebout, D. Scholl, and S. Kirby, pp. 195-214, Amer. Geophys. Union, Washington, D.C., 1996.

Kolarsky, R.A., P. Mann, and W. Montero, Island arc response to shallow subduction of the Cocos Ridge, Costa Rica, in *Geologic and tectonic development of the Caribbean Plate boundary in southern Central America; Special Paper - Geological Society of America*, edited by P. Mann, pp. 235-262, Geol. Soc. Amer., Boulder, 1995.

Kusky, T.M., and C.P. Young, Emplacement of the Resurrection Peninsula ophiolite in the southern Alaska forearc during a ridge-trench encounter, J. Geophys. Res., 104, 29025-29054, 1999.

Li, X.Q., and J.L. Nabelek, Deconvolution of teleseismic body waves for enhancing structure beneath a seismometer array, *Bull. Seismol. Soc. Amer.*, *89*, 190-201, 1999.

Llenos, A.L. and D.H. Christensen, Determination of crustal thickness in Alaska using receiver functions, *EOS Trans. AGU, 84(46),* Fall Meet. Suppl., Abstr. ED41B-1163, 2003.

Matsuzawa, T., N. Umino, A. Hasegawa, and A. Takagi, 1986. Upper mantle velocity structure estimated from PS-converted wave beneath the north-eastern Japan Arc, *Geophys. J. R. astr. Soc.*, *86*, 767-787.

McNamara, D.E., Frequency dependent Lg attenuation in south-central Alaska, *Geophys. Res. Lett.*, *27*, 3949-3952, 2000.

McNamara, D., J. Rubenstein, R. Hansen, and D.H. Christensen, 1999. Lg Attenuation Characteristics in Continental Alaska*, EOS, 80*, 657. (Fall AGU 1999)

Meyers, E.V., D.H. Christensen, and R. Hansen, 1999a. Broadband (Seismic) Experiment Across the Alaska Range (BEAAR) The Alaska Geological Society, Science and Technology Conference, April 23-24, 1999. (AGS meeting, 1999)

Meyers, E.V., D.H. Christensen, R. Hansen, and G. Abers, 1999b. Broadband Experiment Across the Alaska Range - BEAAR, 11th Annual IRIS Workshop at Tenaya Lodge at Yosemite, June 9-12, 1999. (IRIS Workshop, 1999)

Meyers, E.V., D.H. Christensen, G. Abers, and M. Pollock, 1999c. Preliminary Results From BEAAR (Broadband Experiment Across the Alaska Range), *EOS, 80*, 711. (Fall AGU 1999)

Meyers, E.V., D.H. Christensen, G.A. Abers, J.C. Stachnik, A.R. Holland, and K.B. Beebe, 2000. Broad and (Seismic) Experiment Across the Alaska Range (BEAAR) to Determine the Crustal and Upper Mantle Structure Beneath Central Alaska, *EOS, 81*, 877.

Meyers, E.V., D.H. Christensen, A. Ferris, G.A. Abers, and A. Lucier, 2001. Crustal Thickness Across the Alaska Range, *EOS, 82*, 47, 1204.

Meyers-Smith, E.V., D. H. Christensen and G. Abers, Moho topography beneath the Alaska Range: Results from BEAAR, *EOS Trans. AGU*, *83(47)*, fall mtg. suppl., Abstr. S52A-1073, 2002.

Mitchell, B.J., Anelastic structure and evolution of the continental crust and upper mantle from seismic surface wave attenuation, *Rev. Geophys.*, *33*, 441-462, 1995.

Molnar, P., and D. Gray, Subduction of continental lithosphere: some constraints and uncertainties, *Geology*, *7*, 58-62, 1979.

Moore, D.E., D.A. Lockner, M. Shengli, R. Summers, and J.D. Byerlee, Strengths of serpentinite at elevated temperatures, *J. Geophys. Res.*, *102*, 14,787-14,801, 1997.

Obara, K., Nonvolcanic deep tremor associated with subduction in southwest Japan, *Science*, *296*, 1679-1681, 2002.

Oleskevich, D., R. Hyndman, and K. Wang, The updip and downdip limits to great subduction earthquakes: Thermal and structural models of Cascadia, south Alaska, SW Japan, and Chile, *J. Geophys. Res.*, *104*, 14965-14991, 1999.

Page, R.A., C.D. Stephens, and J.C. Lahr, Seismicity of the Wrangell and Aleutian Wadati-Benioff zones and the North America plate along the Trans-Alaska crustal transect, Chugach mountains and Copper River basin, southern Alaska, *J. Geophys. Res.*, *94*, 16059-16082, 1989.

Page, R.A., J.C. Lahr, C.D. Stephens, K.A. Fogleman, T.M. Brocher, and M.A. Fisher, 1992. Seismicity and Stress Orientation in the Alaska Subduction Zone after the Great 1964 Earthquake and Speculation on the Origin of a Giant Asperity, Wadati Conference on Great subduction Earthquakes, Sept, 16-19, 1992, 31-32.

Page, R.A., N.N. Biswas, J.C. Lahr, and H. Pulpan, Seismicity of continental Alaska, in *Neotectonics of North America,*, edited by D.B. Slemmons, E.R. Engdahl, M.D. Zoback, and D.D. Blackwell, pp. 47-68, Geol. Soc. Am., Boulder Colo., 1991.

Parkin, E. J., Horizontal crustal movements determined from surveys after the Alaskan Earthquake of 1964, *The Prince William Sound, Alaska, Earthquake of 1964 and Aftershocks, U.S. Dept. of Comm. Coast and Geodetic Survey, vol. III.*, 1969.

Pavlis, G.L., Imaging the earth with passive seismic arrays, *The Leading Edge*, *22*, 224-231, 2003.

Peacock, S.M., and R.D. Hyndman, 1999. Hydrous minerals in the mantle wedge and the maximum depth of subduction thrust earthquakes, *Geophys. Res. Lett.*, *26*, 2517-2520.

Plafker, G., J.C. Moore, and G.R. Winkler, Geology of the southern Alaska margin, in *The Geology of Alaska, The Geology of North America, G-1,*, edited by G. Plafker, and H.C. Berg, pp. 389-449, Geol. Soc. Am., Boulder, Colorado, 1994.

Protti, M., K. McNally, J. Pacheco, V. Gonzalez, C. Montero, J. Segura, J. Brenes, V. Barboza, E. Malavassi, F. Gueendel, G. Simila, D. Rojas, A. Velasco, A. Mata, and W. Schillinger, The March 25, 1990 (M_W = 7.0, M_L = 6.8), earthquake at the entrance of the Nicoya Gulf, Costa Rica; its prior activity, foreshocks, aftershocks, and triggered seismicity, *J. Geophys. Res.*, *100*, 20,345-20,358, 1995.

Ranero, C., J. Morgan, K. McIntosh, and C. Reichert, Bending-related faulting and mantle serpentinization at the Middle America trench, *Nature*, *425*, 367-373, 2003.

Ratchkovski, N., and R. Hansen, New evidence for segmentation of the Alaska subduction zone, *Bull. Seismol. Soc. Amer.*, *92*, 1754-1765, 2002.

Ratchkovski, N.A., J. Pujol, and N.N. Biswas, 1998. Relocation of Shallow Earthquakes in Southern Alaska Using Joint Hypocenter Determination Method, *Journal of Seismology*, *2*, 87-102.

Revenaugh, J., 1995. A scattered-wave image of subduction beneath the Transverse Ranges, *Science*, *268*, 1888-1892.

Rogers, G., and H. Dragert, Episodic tremor and slip on the Cascadia subduction zone: The chatter of silent slip, *Science*, *300*, 1942-1943, 2003.

Rondenay, S., M.G. Bostock, and J. Schragge, 2001. Multiparameter two-dimensional inversion of scattered teleseismic body waves, 3, Application to the Cascadia 1993 data set, *J. Geophys. Res.*, *106*, 30,795-30,808.

Roth, E.G., D.A. Wiens, and D. Zhao, 2000. An empirical relationship between seismic attenuation and velocity anomalies in the upper mantle, *Geophys. Res. Lett., 27*, 601-604.

Rudnick, R.L., and D.M. Fountain, Nature and composition of the continental crust; a lower crustal perspective, *Rev. Geophys., 33*, 267-309, 1995.

Ruff, L.J., and H. Kanamori, 1983. The Rupture Process and Asperity Distribution of Great Earthquakes from Long-period Diffracted P waves, *Phys. Earth Planet. Inter., 31*, 202-230.

Rüpke, L.H., J.Phipps-Morgan, M. Hort, and J.A.D. Connolly, Are the regional variations in Central American arc lavas due to differing basaltic versus peridotitic slab sources of fluids?, *Geology*, *30*, 1035-1038, 2002.

Saleeby, J.B., Accretionary tectonics of the North American Cordillera, *Ann. Rev. Earth Planet. Sci.*, *15*, 45-73, 1983.

Schermer, E.R., D.G. Howell, and D.L. Jones, The origin of allochthonous terranes, *Ann. Rev. Earth Planet Sci.*, *12*, 107-131, 1984.

Scholz, C.H., 1998. Earthquakes and friction laws, *Nature*, *391*, 37-42.

Schwab, W.C., T.R. Bruns, and R. von Huene, 1980. Maps Showing Structural Interpretation of Magnetic Lineaments in the Northern Gulf of Alaska, Scale 1:1,500,000, U.S. Geol. Surv. Misc. Field Stud. Map, MF-1245.

Searcy, C., and D.H. Christensen, 1994. Tomographic Inversion of Teleseismic P-Wave Data for the Crust and Upper Mantle Structure Beneath Alaska, *EOS*, 75, 450. (Fall AGU 1994)

SEIZE (Seismogenic Zone) Science Plan (rev.), 2003. U.S. MARGINS Program, http://www.margins.wustl.edu/margins/SEIZE/SEIZE-Plan5.pdf.

Sheehan, A.F., P.M. Shearer, H.J. Gilbert, and K.G. Dueker, 2000. Seismic migration processing of P-SV converted phases for mantle discontinuity structure beneath the Snake River Plain, western United States, *J. Geophys. Res.*, *105*, 19,055-19,065.

Sisson, V.B., and T.L. Pavlis, Geologic consequences of plate reorganization: an example from the Eocene southern Alaska fore arc, *Geology*, *21*, 913-916, 1993.

Stachnik, J.C., Seismic attenuation in central Alaska, MA thesis, Boston University, Boston, 2002.

Stachnik, J., G. Abers, and D.H. Christensen, 1999. The Broadband Experiment Across the Alaska Range (BEAAR) Project: A Preliminary Report of Local Earthquake From an IRIS Intern Perspective, *EOS, 80*, 46, 725. (Fall AGU 1999)

Stachnik, J., G. Abers, D. Christensen, E.V. Meyers, 2001. Balance of Alaska Range Topography Through Elevated Mantle Wedge Temperatures, as Estimated by Seismic Attenuation, *EOS, 82*, 271. (Spring AGU 2001)

Stachnik, J.C., G.A. Abers, and D.H. Christensen, 2002a. Seismic Attenuation and Source Scaling from Intermediate-depth Earthquakes: BEAAR Results from Central Alaska, *Seism. Res. Lett, 73*, 2, 233. (SSA 2002)

Stachnik, J., G.A. Abers and D.H. Christensen, Mantle wedge temperature estimates and implications for wedge melting from seismic attenuation beneath Central Alaska: Results from BEAAR, *EOS Trans. AGU*, *83(47)*, fall mtg. suppl., Abstr. S52A-1069, 2002b.

Stachnik, J.C., Abers, G.A., and D.Christensen, Seismic attenuation and mantle temperature in the Alaska subduction zone*, for J. Geophys. Res.*, *in internal review,* 2003.

Stephens, C.D., R.A. Page, and J.C. Lahr, 1990. Reflected and Mode-Converted Seismic Waves Within the Shallow Aleutian Subduction Zone, Southern Kenai Peninsula, Alaska*, J. Geophy. Res., 95*, 6883-6897.

Stroujkova, A.F. and P.E. Malin, A Magma Mass beneath Casa Diablo? Further Evidence from Reflected Seismic Waves, *Bull. Seismol. Soc. Amer., 90,* 500-511, 2000.

Suyehiro, K., N. Takahashi, Y. Ariie, Y. Yokoi, R. Hino, M. Shinohara, T. Kanazawa, N. Hirata, H. Tokuyama, and A. Taira, Continental crust, crustal underplating, and low-Q upper mantle beneath an oceanic island arc, *Science*, *272*, 390-392, 1996.

Tarantola, A., and B. Valette, Inverse problems = Quest for information, *J. Geophys.*, *50*, 159-170, 1982.

Taylor, S.R., and S.M. McLennan, *The Continental Crust: its Composition and Evolution*, 312 pp., Blackwell, Oxford, 1985.

Thurber C, Roecker, S, Roberts, K, Gold, M, Powell, L, and Rittger, K, Earthquake locations and three-dimensional fault zone structure along the creeping section of the San Andreas fault near Parkfield, CA: Preparing for SAFOD, *Geophys. Res. Lett.*, *30* (3), Art. no. 1112, 2003.

Tichelaar, B.W., and L.J. Ruff, 1993. Depth of seismic coupling along subduction zones, *J. Geophy. Res.*, *98*, 2017-2037.

Vernon, F., J. Eakins and R. Newman, Bigfoot Deployment as of January 2002, Earthscope/USArray, http://www.earthscope.org/usarray/usarray_assets/USArray6.mov, 2002.

Vidale, J.E., 1990. Finite-difference calculation of traveltimes in three dimensions, *Geophysics*, *55*, 521-526.

von Huene, R., D. Klaeschen, J. Fruehn, J.E. Sauber, and R.E. Dmowska, 1999. Relation between the subducting plate and seismicity associated with the great 1964 Alaska earthquake, *Pure Appl. Geophys.*, *154*, 575-591.

Waldhauser, F., and W.L. Ellsworth, 2000. A Double-Difference Earthquake Location Algorithm: Method and Application to the Northern Hayward Fault, California*, Bull. Seism. Soc. Am., 90*, 1353-1368.

Wiens, D.A., and G.P. Smith, 2003. Seismological constraints on structure and flow patterns within the mantle wedge, in AGU Monograph, Inside the Subduction Factory, edited by J. Eiler, in press.

Yuan, X., S.V. Sobolev, R. Kind, O. Oncken, G. Bock, G. Asch, B. Schurr, F. Graeber, A. Rudloff, W. Hanka, K. Wylegalla, R. Tibi, C. Haberland, A. Rietbrock, P. Giese, P. Wigger, P. Rower, G. Zandt, S. Beck, T. Wallace, M. Pardo, and D. Comte, 2000. Subduction and collision processes in the Central Andes constrained by converted seismic phases, *Nature*, *408*, 958-961.

Zhao, D., D.H. Christensen, and H. Pulpan, 1995. Tomographic Imaging of the Alaska Subduction Zone, *J. Geophys. Res., 100*, 6487-6504.

Zhu, L., 2000. Crustal structure across the San Andreas Fault, southern California from teleseismic converted waves, *Earth and Planet. Sci. Lett.*, *179*, 183-190.

Zweck, C., J. T. Freymueller, and S. C. Cohen, Elastic dislocation modeling of the postseismic response to the 1964 Alaska Earthquake, *J. Geophys. Res.*, 2001JB000409, 2002a.

Zweck, C., J. T. Freymueller, and S. C. Cohen, The 1964 Great Alaska Earthquake: Present Day and Cumulative Postseismic Deformation in the Western Kenai Peninsula, *PEPI*, 132, 5-20, 2002b.